

## ENHANCING THE FLIGHT SIMULATOR FEELING BY A MINIMISING BACKLASH-EFFECTS PROCESS

Z. Amara, J. Bordeneuve-Guibé, C. Bérard

*Université de Toulouse - Institut Supérieur de l'Aéronautique et de l'Espace (ISAE)  
10, avenue E. Belin, 31055 Toulouse, France  
joel.bordeneuve@isae.fr*

---

**Abstract:** In this paper we addressed the problem of improving the control of AC motors used for the specific application of 3 degrees of freedom moving base flight simulator. Indeed the presence of backlash in DC motors gearboxes induces shocks and naturally limits the flight feeling. A comparison is hence set up between two techniques aiming to deal with this problem: Adaptive Fuzzy Controller and Neural Controller. Dynamic inversion with Fuzzy Logic is used to design an adaptive backlash compensator. The classification property of fuzzy logic techniques makes them a natural candidate for the rejection of errors induced by the backlash. A tuning algorithm is given for the fuzzy logic parameters, so that the output backlash compensation scheme becomes adaptive. The compensator uses the Neural Networks techniques demonstrate that artificial neural networks can be used to compensate hysteresis caused by gear backlash in precision position-controlled mechanisms. A major contribution of this research is that physical analysis of the system nonlinearities and optimal control are used to design the neural network structure.

---

### 1. INTRODUCTION

This new kind of simulator, which is developed by the 6Mouv company ([www.6mouv.com](http://www.6mouv.com)), is actually the matter of an industry-university partnership between 6Mouv and ISAE. Its innovative characteristic relies on a low cost mechanical system that allows the cabin to move around 3, 4 or even 6 degrees of freedom. Basically, in comparison with classical solutions, this one makes use of electrical drives instead of hydraulic actuators.

The motion based is based on rotary asynchronous AC motors using standard rod-crank systems, which appears to be much robust and cheaper than screw or hydraulic jack's solutions. The output force can be very large when using a high ratio gearbox and a powerful motor.

Gearbox are used to convert the high speed - low torque output of the motor into a lower speed - higher torque input to the receiving organ. The main disadvantages of this transmission system consist of the backlash nonlinearity which is caused by the difference between tooth space and tooth width in mechanical system. Any amount of backlash greater than the minimum amount necessary to ensure satisfactory meshing of gears can result in instability in dynamics situations and position errors in gear trains. The backlash nonlinearity will not only increase the static error of the system but also affect its performance.

Under step input, it will make the setting time of system longer, the number of oscillation times greater, and will even result in a non-attenuated sustained oscillation. Backlash is particularly common in actuators, such as mechanical connections, hydraulic servo valves and electric servomotors. To reduce the effect of this nonlinearity several methods are developed in the literature, consisting on: exerting a continue action on the machine output shaft to force the contacts

between gear's teeth. The contact point being then unknown, the mechanism is in constant thrust, whatever the rotation. Instead of exerting a force to diminish the backlash, it is also possible to verify if there is indeed contact between the gearbox teeth and to act in consequence.

The backlash can also be mechanically coped by adding a second torque, opposed to the main movement, but of lower intensity. In other words, that means placing a secondary motor on the reducers' output shaft and making it turn in opposite direction, thus rendering the final solution "very" expensive.

A spiral spring could also exert a permanent contact action, (Slotine E. and Li W., 1991), (Seidl R., 1993), (Seidl R., 1996). The drawbacks of such a solution are on one hand that this action - being permanent - causes useless energy consumption, and on the other hand it remains impossible to adapt or to change the intensity during the run. The "ideal" solution would be to overlook mechanical systems and to find a way of reaching accurate positioning using only one control law.

### 2. ADAPTIVE FUZZY CONTROLLER – DYNAMIC INVERSION

In this part, we present a simple iterative learning control scheme that can be applied for a broad class of nonlinear systems. The tracking capability of the iterative learning process hinges upon the stability of the closed-loop system at each iteration.

The fuzzy controller to be tuned is a feed-forward controller (fig.1). This fuzzy controller can be seen as a one-step-ahead controller which is identical with the inverse process model. In the proposed control architecture the gradient-descent

method is used to learn the inverse model of the plant by changing the parameters of the fuzzy part of the inverse model.

2.1. Gradient-descent adaptation

More and more references to “fuzzy neural networks” or “neuro-fuzzy systems” can be found in the literature. A few of them really use neural networks initialized by a fuzzy rule base. Examples can be found in (Shimojima I. and Fukuda T., 2005), (Harris C.J and Moore C.G., 2002), (Harris C.J and Moore C.G., 1993) and (Horikawa S., Furuhashi T., 1993), where a fuzzy system is first translated into a neural network and then used to learn a model. Most of the publications on fuzzy neural networks address the adaptation of fuzzy systems based on a gradient-descent adaptation method for optimization (Guely F., Siarry P., 2000). However, the gradient-descent adaptation technique is not specific to neural networks. Several authors have applied gradient-descent adaptation methods to fuzzy systems. What those methods have in common is that they minimize a similar objective function *E* as it is done in case of the learning rules in neural networks, as well as in many other gradient-descent optimization methods:

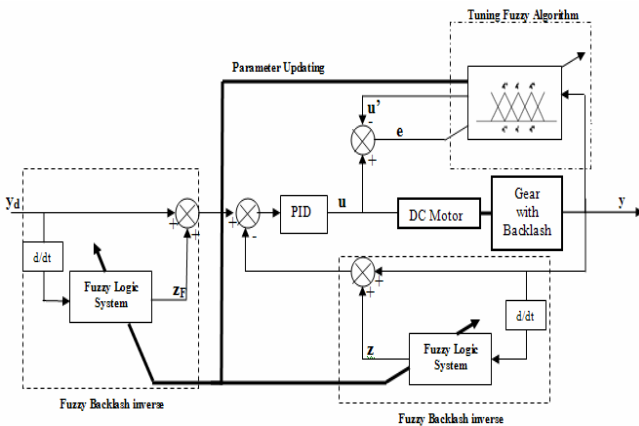


Fig. 1. Fuzzy output backlash compensation.

$$E = \frac{1}{2}(y - y_d)^2 \tag{1}$$

where  $y_d$  is the reference for the fuzzy system output  $y$ .

2.2. The adaptation scheme

We consider triangularly-shaped membership functions for the inputs, Sugeno rules with constant consequent and the product operator for conjunction. The rules have the following form (Slotine E. and Li W., 1991):

$$L^{i,j} : IF y(k+1) \text{ is } A_1^i \text{ and } y(k) \text{ is } A_2^j \text{ THEN } u(k) = b^{i,j} \tag{2}$$

Where  $L^{i,j}$  denote the  $i,j$ -th implication,  $i = 1, 2, \dots, N_i$ ,  $j = 1, 2, \dots, N_j$  and  $N_j$  are the number of the fuzzy sets on the  $i$ -th and  $j$ -th input domain, respectively; the symbol  $A_q^i$  and

$A_q^i$  are the membership functions and  $b^{i,j}$  are the rule consequent parameters (Fuzzy singleton).

2.3. The control problem

A fuzzy backlash inverse compensator is designed for the no symmetric output backlash nonlinearity. The output backlash example is shown in fig.2. The backlash characteristic  $F(\square)$  with input  $z(t)$  and output  $y(t) : y(t) = F[z(t)]$  is described by two parallel straight lines, upward and downward sides of  $F(\square)$ , connected with horizontal line segments. Mathematically, the backlash is modelled as (5), (Jang J. O., 2000):

$$y = F(y, z, z) = \begin{cases} z(t), & \text{IF } z(t) > 0 \text{ AND } y(t) = z(t) - d_+ \\ \text{OR } z(t) < 0 \text{ AND } y(t) = z(t) - d_- \\ 0, & \text{otherwise} \end{cases} \tag{5}$$

A graphical inverse of the backlash characteristic is shown in fig.3, which contains vertical jumps. The mapping  $FI(\square)$ :

$$y_d(t) \rightarrow z_d(t), \text{ define the backlash inverse } F(FI(y_d(\tau))) = y_d(\tau) \Rightarrow F(FI(y_d(t))) = y_d(t) \text{ for any } \tau > t.$$

Because of the dynamic nature of backlash, the backlash inverse is defined with the initialization

$$F(FI(y_d(t))) = y_d(\tau).$$

To offset the deleterious effects of backlash, we introduce the idea of the fuzzy backlash inverse scheme in fig.3. A fuzzy backlash inverse compensator using dynamic inversion would be discontinuous and would depend

on the region within which  $y_d$  occurs. It would be naturally described using the rules (6):

$$\begin{aligned} IF (y_d > 0) & \text{ THEN } (z_d = y_d + \hat{d}_+) \\ IF (y_d = 0) & \text{ THEN } (z_d = y_d + \hat{d}_0) \\ IF (y_d < 0) & \text{ THEN } (z_d = y_d + \hat{d}_-) \end{aligned} \tag{6}$$

Where  $\hat{d} = [\hat{d}_+ \ \hat{d}_0 \ \hat{d}_-]^T$  is an estimate of the backlash with

parameter vector  $d = [d_+ \ d_0 \ d_-]^T$ .  $d_0$  is determined by:

$$\begin{aligned} \hat{d}_0 &= \hat{d}_+ \text{ if } y(t-1) > 0 \\ \hat{d}_0 &= \hat{d}_- \text{ if } y(t-1) < 0 \end{aligned} \tag{7}$$

To make this intuitive notion (7) mathematically precise for analysis, let's define the membership functions,

$$X_+(y_d) = \begin{cases} 0, & y_d < 0 \\ 1, & y_d > 0 \end{cases}, X_0(y_d) = \begin{cases} 0, & y_d \neq 0 \\ 1, & y_d = 0 \end{cases}, X_-(y_d) = \begin{cases} 0, & y_d < 0 \\ 1, & y_d > 0 \end{cases}$$

One may write the inverse compensator as:

$$z_d = y_d + z_F \quad (8)$$

where  $z_F$  is given by the rule base

$$\begin{aligned} \text{IF } (y_d \in X_+(y)) \quad \text{THEN } (z_F = \hat{d}_+) \\ \text{IF } (y_d \in X_0(y)) \quad \text{THEN } (z_F = \hat{d}_0) \\ \text{IF } (y_d \in X_-(y)) \quad \text{THEN } (z_F = \hat{d}_-) \end{aligned} \quad (9)$$

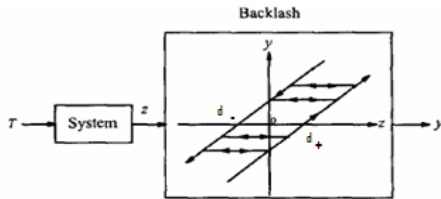


Fig. 2. System with output backlash.

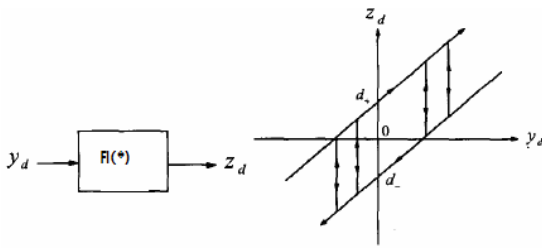


Fig. 3. Backlash inverse.

The output of the fuzzy logic system with this rule base is given by

$$z_F = \frac{\hat{d}_+ X_+(y_d) + \hat{d}_0 X_0(y_d) + \hat{d}_- X_-(y_d)}{X_+(y_d) + X_0(y_d) + X_-(y_d)} \quad (10)$$

The estimates  $\hat{d}_+, \hat{d}_0, \hat{d}_-$  are respectively, the control representative value of  $X_+(y_d), X_0(y_d)$  and  $X_-(y_d)$ . This may

be written (note  $X_+(y_d) + X_0(y_d) + X_-(y_d) = 1$ ) as :

$$z_F = \hat{d}^T X(y_d) \quad (11)$$

where the fuzzy logic basis function vector given by :

$$X(y_d) = \begin{bmatrix} X_+(y_d) \\ X_0(y_d) \\ X_-(y_d) \end{bmatrix} \quad (12)$$

is easily computed given any value of  $y_d$ . It should be noted that the membership functions are the indicator functions and  $X(y_d)$  is similar to the regressor.

The fuzzy backlash inverse compensator may be expressed as follows :

$$z_d = y_d + z_F = y_d + \hat{d}^T X(y_d) \quad (13)$$

where  $\hat{d}$  is the estimated backlash width.

Since  $z(t)$  is not available, we choose its estimate to be :

$$\bar{z}(t) = y(t) + \bar{z}_F = y + \hat{d}^T X(y) \quad (14)$$

where the fuzzy basis function vector given by :

$$X(y) = \begin{bmatrix} X_+(y) \\ X_0(y) \\ X_-(y) \end{bmatrix} \quad (15)$$

is easily computed given any value of  $y$ .

### 3. NEURAL CONTROLLER

#### 2.1. The backlash model

The state equations describing backlash hysteresis are given by (16)-(28). The subscripts M and L denote motor and load shaft quantities. The time dependent variables are angular acceleration ( $\alpha$ ), velocity ( $\omega$ ), position ( $\theta$ ), and torque ( $\tau$ ) (Slotine E. and Li W., 1991), (Seidl R., 1993).

The torque terms are the motor air gap torque ( $\tau_M$ ), the friction torques ( $\tau_{FM}$  and  $\tau_{FL}$ ) and the torque transmitted through the gear to the load shaft ( $\tau_G$ ). The physical constants are the inertias ( $J_M$  and  $J_L$ ), the viscous ( $B_M$  and  $B_L$ ), coulomb ( $C_M$  and  $C_L$ ), and static ( $S_M$  and  $S_L$ ) friction values, the gear ratio ( $R$ ) and half of the angular dead zone distance between gears on the motor shaft side ( $\sigma$ ). The friction torques (20, 21) and gear transmission torque (22) are functions of the state ( $\omega_M, \theta_M, \omega_L$ , and  $\theta_L$ ) and the input ( $\tau_M$ ) and receive their time dependence through these variables. The time dependence and state dependence designations are omitted for conciseness except when needed. Time instants just before and after time  $t$  are denoted  $t^-$  and  $t^+$ .

$$\frac{d\omega_M}{dt} = J_M^{-1} [-\tau_{FM} - R\tau_G + \tau_M] \quad (16)$$

$$\frac{d\theta_M}{dt} = \omega_M \quad (17)$$

$$\frac{d\omega_L}{dt} = J_L^{-1} [-\tau_{FL} + \tau_G] \quad (18)$$

$$\frac{d\theta_L}{dt} = \omega_L \quad (19)$$

Where:

$$\begin{aligned} \tau_{FM} = -B_M \omega_M - C_M \text{sgn}(\omega_M) \\ - \text{sgn}(\tau_M - R\tau_G) \min(|S_M|, |\tau_M - R\tau_G|) 1\{\omega_M = 0\} \end{aligned} \quad (20)$$

$$\tau_{FL} = -B_L \omega_L - C_L \text{sgn}(\omega_L) - \text{sgn}(\tau_L) \min(|S_L|, |\tau_G|) 1\{\omega_L = 0\} \quad (21)$$

$$\tau_G = \tau_D + \tau_{PM} + \tau_{NM} + \tau_{PS} + \tau_{NS} + \tau_{PI} + \tau_{NI} \quad (22)$$

$$\tau_D = 0 \cdot 1\{-\sigma < \theta_M - R^{-1}\theta_L < \sigma\} \quad (22)$$

$$\tau_{PM} = \max(0, (J_M + R^2 J_L)^{-1} [R J_L (\tau_M - \tau_{FM}) + J_M \tau_{FL}]) \cdot 1\{\theta_M - R^{-1}\theta_L = \sigma \cap \omega_M = R^{-1}\omega_L \neq 0\} \quad (23)$$

$$\tau_{NM} = \min(0, (J_M + R^2 J_L)^{-1} [R J_L (\tau_M - \tau_{FM}) + J_M \tau_{FL}]) \cdot 1\{\theta_M - R^{-1}\theta_L = -\sigma \cap \omega_M = R^{-1}\omega_L \neq 0\} \quad (24)$$

$$\tau_{PS} = \max(0, \tau_M - S_M) \cdot 1\{\theta_M - R^{-1}\theta_L = \sigma \cap \omega_M = R^{-1}\omega_L \neq 0\} \quad (25)$$

$$\tau_{NS} = \min(0, \tau_M + S_M) \cdot 1\{\theta_M - R^{-1}\theta_L = -\sigma \cap \omega_M = R^{-1}\omega_L \neq 0\} \quad (26)$$

$$\tau_{PI} = J_M J_L (J_M + R^2 J_L)^{-1} (R \omega_M(t^-) - \omega_L(t^-)) \cdot \delta\{\theta_M - R^{-1}\theta_L = \sigma \cap \omega_M(t) > R^{-1}\omega_L(t)\} \quad (27)$$

$$\tau_{NI} = J_M J_L (J_M + R^2 J_L)^{-1} (R \omega_M(t^-) - \omega_L(t^-)) \cdot \delta\{\theta_M - R^{-1}\theta_L = -\sigma \cap \omega_M(t) < R^{-1}\omega_L(t)\} \quad (28)$$

The state equations (16)-(19) describe the motor and load shaft velocities and positions. Both shafts include friction torques described in (20) and (21). The friction models include viscous, coulomb and static terms. The gear torque described in (22) acts on the output shaft and the reflected gear torque react on the motor shaft. The expression for gear torque has several terms. Boolean function, used in (23)-(26), equals "1" when the bracketed condition is true, causing acceleration impulses and velocity step changes. All achievable state conditions are covered by these mutually exclusive terms.

## 2.2. The controller

In equation (29)-(30), \* denotes desired, command or reference, ^ denotes estimated, ~ denotes error and  $\hat{\wedge}$  denotes estimation error.

The load shaft control:

$$\tau_G^* \cong \hat{J}_L \alpha_L^* + \hat{\tau}_{FL} + B_{AL} \left( \omega_L^* - \hat{\omega}_L \right) + K_{AL} \left( \theta_L^* - \hat{\theta}_L \right) \quad (29)$$

The motor shaft control:

$$\tau_M \cong \hat{J}_M \alpha_M^* + \hat{\tau}_{FM} + B_{AM} \left( \omega_M^* - \hat{\omega}_M \right) + K_{AM} \left( \theta_M^* - \hat{\theta}_M \right) + R \tau_G^* + N \tau_G^* \quad (30)$$

The relative trajectory control:

$$\Theta \approx \sigma \text{sgn}(\tau_G^*) \quad \Omega \cong \eta \cdot \text{sgn}(\tau_G^*) \quad \eta \cong 0 \quad (31)$$

$$SC \cong \Theta + (2A)^{-1} (\Omega^2 - \omega_R^{*2}) \cdot [1\{\omega_R^* \leq \Omega\} - 1\{\omega_R^* \geq \Omega\}] \quad (32)$$

$$\alpha_R^* \cong A \cdot [1\{\theta_R^* \leq SC\} - 1\{\theta_R^* \geq SC\}] - [\Omega \cdot (\delta\{\theta_R^* = +\sigma \wedge \omega_R^* > 0\} + \delta\{\theta_R^* = -\sigma \wedge \omega_R^* < 0\})] \quad (33)$$

$$\alpha_R^* \in [-A, A] \quad (34)$$

$$\omega_R^* \approx \omega_R^*(0) + \int_0^t \alpha_R^*(t) \partial t \quad (35)$$

$$\theta_R^* \approx \theta_R^*(0) + \int_0^t \omega_R^*(t) \partial t \quad (36)$$

$$\alpha_M^* \approx R^{-1} \hat{\alpha}_L + \alpha_L^* \quad (37)$$

The gear torque controller:

$$\tau_G = \tau_G^* R^{-1} \cdot 1\{[\theta_R^* = \sigma \cap \tau_G^* > 0] \cup [\theta_R^* = -\sigma \cap \tau_G^* < 0]\} \quad (38)$$

Since relative motion of the shafts makes backlash representation easier,  $\theta_R = \theta_M - R^{-1}\theta_L$  is used to simplify the equations.

Only state variable estimates are used to avoid specifying a priori which variables are measured and which are estimated using desired or observed values. The controller's objective is to make the load shaft follow a desired position trajectory by generating the appropriate motor shaft torque command and reference trajectory. To do this, the gear torque needed to cause the load shaft to follow the desired trajectory is calculated. Then a motor shaft reference trajectory is generated that uses time-optimal control to guide the motor shaft to (and then hold the shaft at) the correct backlash boundary, making it possible to apply the desired gear torque. Then the motor torque is computed that decouples the motor shaft dynamics, provides state error feedback and, if the gear is engaged, supplies the desired gear torque. The switching condition/curve SC is the solution to minimizing the time required to reach a given  $\omega_R^*(t_f) = \Theta$  with  $\omega_R^*(t_f) = \Omega = 0$  subject to  $\alpha_R^* \in [-A, A]$ . By setting  $\theta_R^*(t_f) = \Theta = \sigma \text{sgn}(\tau_G^*)$  in (4.i), the final relative position is the middle of the backlash region if  $\tau_G^* = 0$  and the proper boundary of the backlash region if  $\tau_G^* \neq 0$ . Thus, the gears are engaged quickly and smoothly with zero relative velocity.

## 2.3. The neural network controller

The direct construction of the backlash neural controller is based on a building block approach that dedicates a neuron or neurons to the realization of each individual controller function. This physical model-based approach is similar in concept to the synthesis of analogue computers as discussed in (Seidl R., 1993), (Rumelhart E., Hinton G. E, and Williams R. J, 2001), (Hod K., Stinchcombe M., and White H., 2005). Many desired control functions, including linear feedback, bang-bang and logical AND and OR, have extremely simple neuron realizations. More complicated functions encountered in nonlinear decoupling can be approximated using a piecewise reconstruction procedure. The neural network controller is detailed in (Amara Z., 2007c) and pictured in Fig. 4.

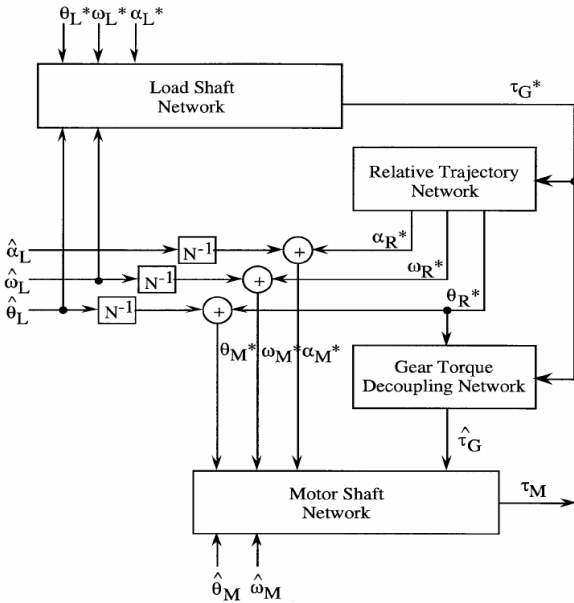


Fig. 4. Backlash neural network controller architecture.

#### 4. SIMULATIONS RESULTS

##### 4.1. Backlash effects

The considered case represents a gearbox with  $0.25^\circ$  (0.004 rad) dead zone distance.

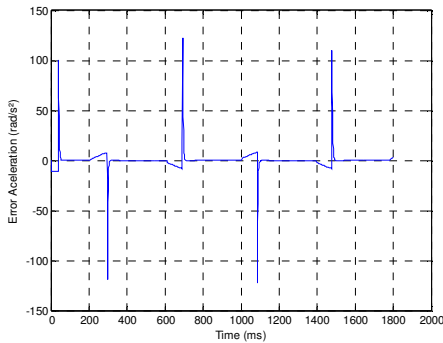


Fig.5. Error: Acceleration (without control).

##### 4.2. Adaptive Fuzzy controller results

The simulation result for on-line identification of backlash parameters are shown in Fig. 6. by using (3), (4) and (9). The result proves the robustness and speed of the Adaptive Fuzzy Algorithm. The Identification parameters are updated online in the Inverse model of the Gear.

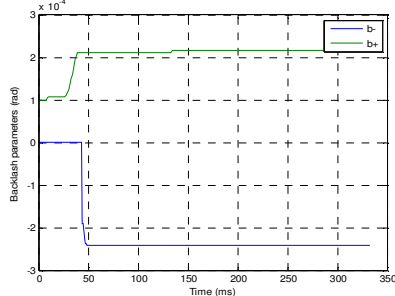


Fig. 6. On-line Identification of backlash parameters.

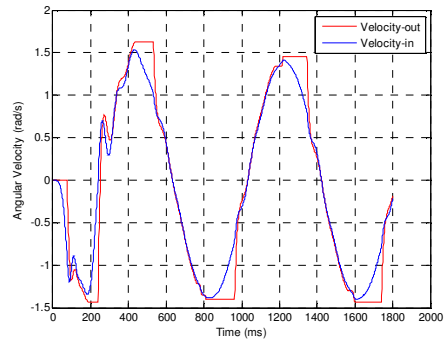


Fig.7. Output and input velocity gearbox.

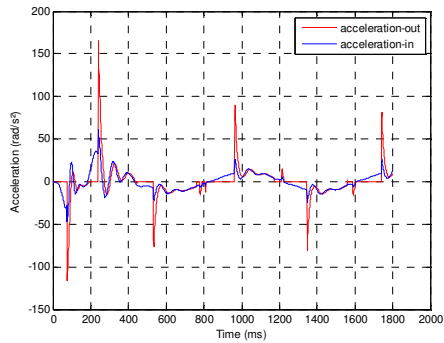


Fig.8. Output and input acceleration gearbox.

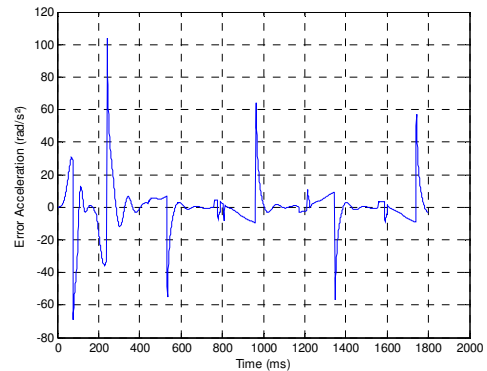


Fig.9. Error: Acceleration.

By comparing Fig.5. and Fig.9, we can observe that adaptive fuzzy controller minimizes the acceleration impulses, which means minimizing shocks and vibrations in the mechanical structure.

The development of inverse dynamics technique makes it possible to command the machine in the opposite backlash dynamic and thus, minimizing the effects caused by this backlash non-linearity. This approach is actually under evaluation in the dynamic simulator command.

4.3. Neural controller results

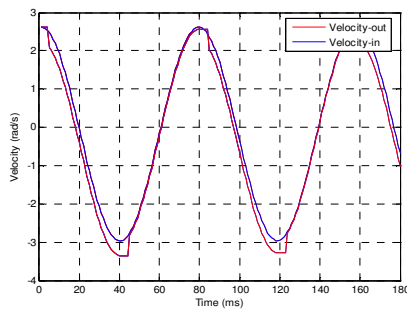


Fig.10. Output and input velocity gearbox.

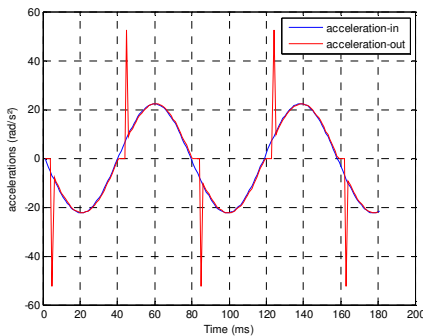


Fig.11. Output and input acceleration gearbox.

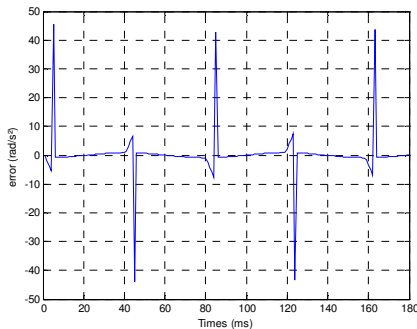


Fig.12. Error: Acceleration.

This study was made within the framework of the dynamic simulator command. The results obtained by simulation, by using Neural Controller, allow minimized effects of the backlash. By comparing Fig.5., Fig.9. and Fig.12, we can observe that Neural Controller results are better than fuzzy controller ones, acceleration impulses are no more intense.

An implementation in real time will be made then. The control algorithm it implements has several unique features:

- It moves the motor shaft to the proper backlash boundary using a time-optimal control subject to acceleration limits.
- Standard linear control is directly implemented by a neuron operating in its linear region. This allows the corresponding weights to be initialized with the gains of an existing controller.
- Logical operations were used to create complicated conditions from basic, single neuron-generated conditions.

5. CONCLUSIONS

In this article, a comparison is performed between two command laws (Adaptive Fuzzy Controller and Neural Controller) in order to minimise backlash effects. The first part discusses the development of a command law based on the inversed dynamic technique thanks to adaptive fuzzy regulator. The second one is reserved for a neural regulator. Simulation results prove the efficiency of the two methods and the effectiveness of the neural regulator in opposition to the adaptive fuzzy regulator.

REFERENCES

Amara Z., Bordeneuve-Guibé J. (2007). Control of new kind of moving base simulator”, Conference on Systems and control. Marrakech, Morocco.

Amara Z., Bordeneuve-Guibé J. (2007). Improvement of flight simulator feeling using Adaptive Fuzzy Controller, in IEEE, Power Control session. Taiwan.

Amara Z., Bordeneuve-Guibé J. (2007). Adaptive Fuzzy Backlash compensation For a New Dynamic Flight Simulator, IFAC AFNC. Valenciennes, France.

Guely F., Siarry P. (1991). Gradient descent method for optimizing various fuzzy rule bases”. IEEE, pp. 1241–1246, 2000.

Horikawa S., Furuhashi T. (1993). On identification of structures in premises of a fuzzy model using a fuzzy neural network ,IEEE pp. 606– 611.

Hod K., Stinchcombe M., and White H., (2005). Multilayer Feed forward networks are universal approximators, Neural Networks, vol.2.

Harris C.J, Moore C.G.( 2002). Intelligent identification and control for autonomous guided vehicles using adaptive fuzzy-based algorithms, Engineering Applications of Artificial Intelligence 2, 267–285..

Harris C.J, Moore C.G. (1993), “Intelligent control - aspects of fuzzy logic and neural nets”,Singapore: World Scientific,.

Jager R., Verbruggen H.B, Adaptive fuzzy control, In Proceedings European Simulation Symposium, Ghent, Belgium, pp. 140–144. SCS.

Jang J. O, (July 2002) Backlash compensation of nonlinear systems using fuzzy logic, Proc. IFAC 151h World Congress.

Rumelhart D. E, Hinton G. E., and Williams R. J., “Learning internal representations by error propagation,” Parallel Distributed Processing. Cambridge, MA: MIT Press, 2001, pp. 45-76. 1967, pp. 128-130.

Slotine J.-J. E., Li W.( 1991) Applied Nonlinear Control Englewood. Cliffs, NJ: Prentice-Hall.

Seidl R. (1995) Neural network compensation of gear backlash hysteresis in position-controlled mechanisms, In Proc IEEE Ind. Applicat, vol.31, N° 6.

Seild R. (1996) .Mention and motor control using neural network , University of WISCONSIN-MADISON.

Shimajima I., Fukuda T. (Oct. 2005), Fuzzy neural networks based on spline functions, in IEEE, Neural Networks session, . Proceedings of International Joint Conference on Volume 1, Issue, 25-29 Page(s): 754 - 757 vol.1